arXiv:1212.5833v1 [cond-mat.quant-gas] 23 Dec 2012

A superheated Bose-condensed gas

Alexander L. Gaunt*, Richard J. Fletcher*, Robert P. Smith†, and Zoran Hadzibabic
Cavendish Laboratory, University of Cambridge, J. J. Thomson Ave., Cambridge CB3 0HE, United Kingdom
(Dated: December 27, 2012)

Our understanding of various states of matter usually relies on the assumption of thermodynamic equilibrium. However, the transitions between different phases of matter can be strongly affected by non-equilibrium phenomena. Here we demonstrate and explain an example of non-equilibrium stalling of a continuous, second-order phase transition. We create a superheated atomic Bose gas, in which a Bose-Einstein condensate (BEC) persists above the equilibrium critical temperature, T_c, if its coupling to the surrounding thermal bath is reduced by tuning interatomic interactions. For vanishing interactions the BEC persists in the superheated regime for a minute. However, if strong interactions are suddenly turned on, it rapidly "boils" away. Our observations can be understood within a two-fluid picture, treating the condensed and thermal components of the gas as separate equilibrium systems with a tuneable inter-component coupling. We experimentally reconstruct a non-equilibrium phase diagram of our gas, and theoretically reproduce its main features.

Non-equilibrium many-body states can persist for a very long time if, for example, a system is integrable, the transition to the lower free-energy state is inhibited by an energy barrier, or the target equilibrium state is continuously evolving due to dissipation. Ultracold atomic gases offer excellent possibilities for fundamental studies of non-equilibrium phenomena [1–12] and have been used to create counter-intuitive states such as repulsively bound atom pairs [3] and Mott insulators with attractive inter-particle interactions [10].

Our superheated Bose gas is reminiscent of superheated distilled water, which remains liquid above 100 °C. Specifically, as the temperature characterising the average energy per particle and the populations of the excited states rises above T_c, the cloud remains in the partially condensed phase, which in true equilibrium should exist only below T_c. However, there are also important differences. Boiling of water is a first-order phase transition and is stalled in clean samples by the absence of nucleation centres. In that case the transition is inhibited by an energy barrier. For a second-order phase transition such a barrier does not exist and the superheating we observe is a purely dynamical non-equilibrium effect, which arises because different properties of the system evolve at different rates. In this respect our gas also bears resemblance to the long-lived non-equilibrium spin structures observed in spinor condensates [4, 7], pre-thermalised states in quenched one-dimensional (1D) Bose gases [12] and supercritical superfluids predicted to occur in quenched 2D gases [13]. In all those cases, however, non-equilibrium states are observed due to the system's *slow approach* to a true equilibrium. Here, the system actually evolves *away* from equilibrium.

In Fig. 1 we summarise the basic idea of our experiments and the key concepts needed to understand them. In an equilibrium gas, a BEC is present only if $T < T_c$, where T_c depends on the total particle number N, or equivalently if the chemical potential is $\mu > \mu_c$. In a standard experiment, after a BEC is produced, it gradually decays because T rises, due to technical heating, and/or T_c decreases, because N decays through various inelastic processes. As T/T_c increases, elastic collisions redistribute the atoms between the thermal and condensed components, aiming to ensure the equilibrium particle distribution. The BEC atom number, N_0, can therefore decay in two ways: (1) by direct inelastic loss, and (2) through elastic transfer of atoms into the thermal component. Here we reduce the rate of the elastic particle transfer by tuning the strength of inter-particle interactions, characterised by the s-wave scattering length a. This protects the BEC deep into the superheated regime, where $N_0 > 0$ even though $T > T_c$.

We can understand our observations within the two-fluid picture outlined in Fig. 1(b). Here we treat the thermal and condensed components as two coupled sub-systems with atom numbers N' and N_0, chemical potentials μ' and μ_0, and instantaneous per-particle inelastic decay rates Γ' and Γ_0, respectively. In equilibrium $\mu' = \mu_0$; note that μ_0 is defined only if $N_0 > 0$, so $\mu_0 > \mu_c$.

The two components are coupled in two ways, both dependent on the scattering length a. First, the local "kinetic" thermal equilibrium between the collective excitations in the BEC (phonons) and the thermal bath is ensured by Landau damping, the rate of which is $\propto \sqrt{a}$ [14–16]. Second, the global "phase" equilibrium (i.e., the equilibrium condensed fraction N_0/N) is ensured by the elastic scattering with a rate $\propto a^2$. Crucially, due to the different scalings with a, we find a large parameter space where the two components can be considered to be in local kinetic equilibrium while the system is not in global phase equilibrium. In other words, the two components are at the same temperature, but have different chemical potentials.

In our optically trapped ^{39}K gas [17], we control a by an external magnetic field tuned close to a Feshbach resonance at 402 G [18], the dominant source of Γ' and Γ_0 is spontaneous scattering of photons from the trapping laser beams, and Γ_0 has an additional contribution from three-body recombination.

The key steps in our experimental sequence are summarised in Fig. 1(c). We start by preparing a partially condensed gas in the $|F, m_F\rangle = |1, 1\rangle$ hyperfine ground state by evaporative cooling at $a = 135\, a_0$, where a_0 is the Bohr radius [17]. We then reduce a (over 50 ms) and follow the subsequent evolution of the cloud, probing the atomic momentum distribution by absorption imaging in time-of-flight expansion. Reducing

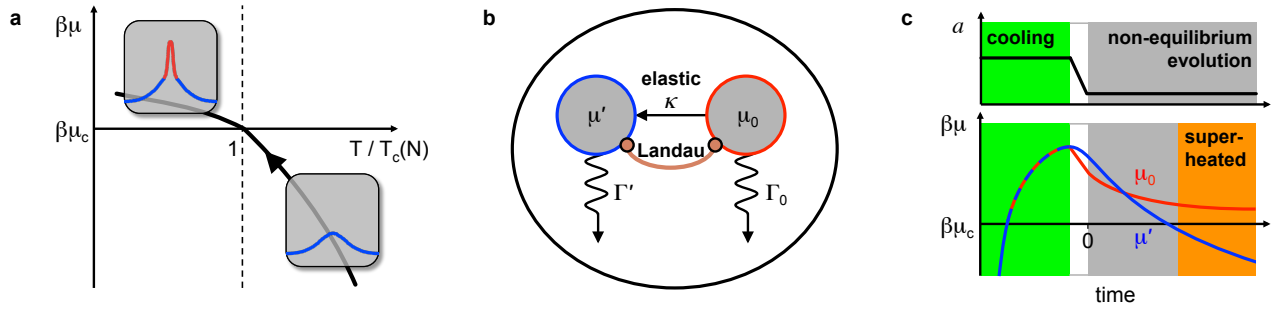

FIG. 1: Creating and understanding a superheated Bose-condensed gas. (a) In equilibrium, a BEC is present if $T < T_c$ or equivalently $\mu > \mu_c$ (here $\beta = 1/(k_B T)$). The arrow indicates the cooling trajectory along which a BEC is produced. The insets show measured momentum distributions, with the condensed component indicated in red. (b) Two-component picture. The thermal and condensed components have chemical potentials μ' and μ_0, and inelastic decay rates Γ' and Γ_0, respectively. The net flow of particles between the two components, κ, depends on μ', μ_0 and the scattering rate $\propto a^2$. In equilibrium $\mu' = \mu_0 = \mu^{\rm eq}$. The Landau damping of the collective modes in the BEC has a rate $\propto \sqrt{a}$. (c) Time-sequence of the experiment. Reducing a after preparing a BEC reduces the coupling between the two components and extends the condensate lifetime. In the superheated regime $\mu' < \mu^{\rm eq} < \mu_c$ but $\mu_0 > \mu_c$.

a (at constant N_0) initially reduces μ_0 below μ' [11], but subsequently μ_0 decays slower.

In Fig. 2 we quantitatively contrast the equilibrium evolution of a cloud at $a = 83\,a_0$ and the non-equilibrium evolution at $5\,a_0$. In both cases we start at time $t = 0$ [see Fig. 1(c)] with $N_0 \approx 2\times10^4$ and $N \approx 2\times10^5$ at $T \approx 160$ nK. In both cases T_c decreases at a similar rate due to similar N-decay. At $5\,a_0$, the temperature rises faster due to less effective evaporative cooling at a fixed optical trap depth.

Whether the gas is in equilibrium or not, it can always be characterised by two *extensive* variables, the total particle number N and energy E. We measure these quantities by direct summation of the momentum distribution and its second moment. To measure N_0 we count the atoms within the central peak rising above the smooth thermal distribution.

From the measured $N(t)$ alone we calculate the equilibrium $T_c(t)$ [19]. From $N(t)$ and $E(t)$ we calculate the equilibrium *intensive* thermodynamic variables $\mu^{\rm eq}(t)$ and $T^{\rm eq}(t)$, and the equilibrium number of condensed atoms, $N_0^{\rm eq}(t)$ [19–21]; in these calculations $N_0^{\rm eq} > 0$ if and only if $T^{\rm eq} < T_c$. For comparison, we also directly fit a temperature T^f to the wings of the momentum distribution. Additionally, supposing only that the two components are separately in equilibrium, from the measured N_0 and N' we calculate μ_0 and μ'. (For theoretical details see Supplementary Information [16].)

At $83\,a_0$ [Fig. 2(a)] we find excellent agreement between the measured N_0 and the $N_0^{\rm eq}$ predicted without any free parameters. The BEC vanishes exactly at the equilibrium "critical time" t_c (dotted green line), at which $T^{\rm eq} = T_c$. Note that the dashed red lines show the experimental bounds on the time $\bar{t}$ when the BEC vanishes. The separately calculated μ_0, μ' and $\mu^{\rm eq}$ are all consistent and we have also checked that the fitted T^f coincides with the calculated $T^{\rm eq}$. All this gives us full confidence in our equilibrium calculations.

At $5\,a_0$ [Fig. 2(b)] we observe strikingly different behaviour. The BEC now survives much longer than it would in true equilibrium; $\bar{t} - t_c \approx 40$ s. We also see that μ_0 and μ' diverge from each other for $t > t_c$, so the system is moving *away* from the global phase equilibrium rather than *towards* it. The observed superheating can thus not be understood as just a transient effect. (Note that $\mu_0 - \mu_c$ is always very small due to weak interactions.)

At $5\,a_0$ the gas is not in global phase equilibrium, but it is still a good approximation to view its two components as two equilibrium sub-systems at a same (kinetic) temperature,

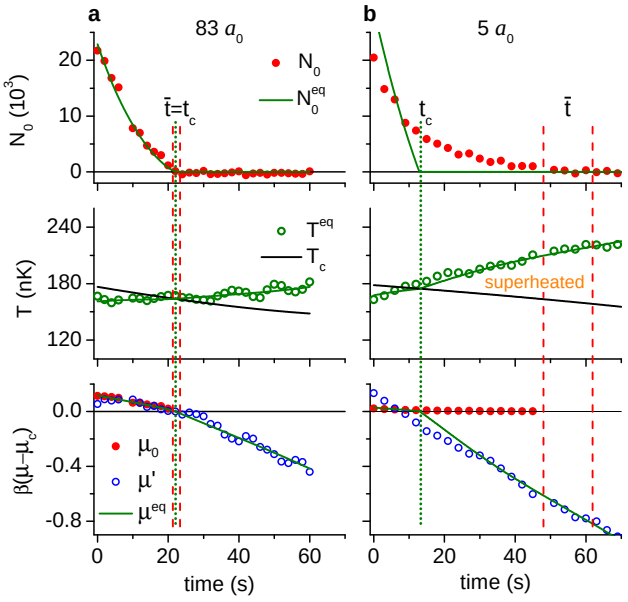

FIG. 2: Equilibrium vs. non-equilibrium BEC decay. (a) At $a = 83\,a_0$ the cloud is always in quasi-static equilibrium. The measured N_0 is in excellent agreement with the predicted $N_0^{\rm eq}$ and vanishes when $T^{\rm eq} = T_c$; the three separately calculated chemical potentials, μ_0, μ' and $\mu^{\rm eq}$, all agree with each other. The dotted green line marks the equilibrium critical time, t_c, and the dashed red lines show the experimental bounds on the time $\bar{t}$ when the BEC actually vanishes. (b) At $5\,a_0$, the BEC persists in the superheated regime ($T^{\rm eq} > T_c$) for $\bar{t} - t_c \approx 40$ s.

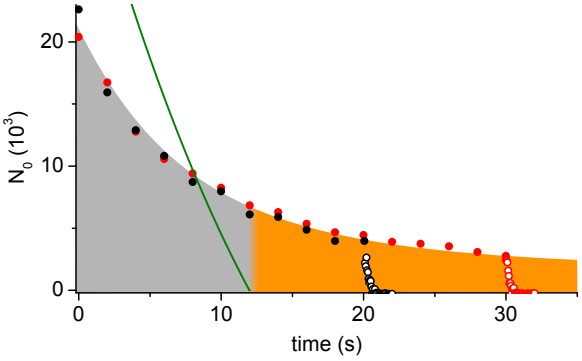

FIG. 3: Quenching the superheated Bose-condensed gas. Solid symbols show the evolution of N_0 at $a = 3\,a_0$, the green solid line shows $N_0^{\rm eq}$ and orange shading indicates the superheated regime. Open symbols show the rapid decay of the BEC after it is strongly coupled to the thermal bath by an interaction quench to $a = 62\,a_0$ at time t_q. We show two experimental series in which $t_q = 20\,$s (black) and 30 s (red).

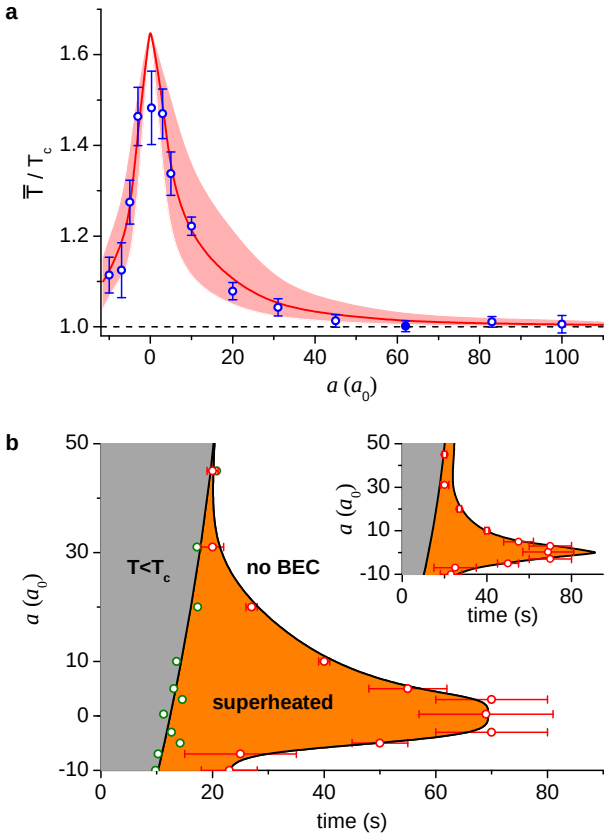

FIG. 4: Limits of superheating. (a) The highest temperature at which we observe a BEC, $\bar{T}$, scaled to the equilibrium T_c. Close to $a = 0$ the BEC survives up to $\approx 1.47\,T_c$. The red line shows the results of our numerical calculations, with the shaded area indicating the theoretical uncertainty. Experimental error bars are statistical. The point at $62\,a_0$ is fixed to unity by the absolute atom number calibration [19, 26]. (b) Temporal phase diagram. For each value of a we plot the equilibrium t_c (green points) and the time $\bar{t}$ at which the BEC actually vanishes (red points). The $\bar{t}$ errors correspond to dashed lines in Fig. 2 and the uncertainty in t_c is indicated by the scatter of points. Solid curves are spline fits to the data. For $a \approx 0$ the BEC survives in the superheated regime for a whole minute. Inset: numerically calculated phase diagram, with $\bar{t}$ data overlaid.

as in Fig. 1(b). We have checked that the momentum distribution in the non-condensed component is still fitted well by a thermal distribution, with T^f always within 10 % of the calculated $T^{\rm eq}(N, E)$ (see Supplementary Information [16]). For the BEC, in a weakly interacting gas the equilibrium relation $\mu_0(N_0)$ relies on the macroscopic occupation of a single quantum state [22], rather than on global equilibrium. Moreover, even for the lowest-energy collective modes we estimate the Landau damping time to be < 1 s [14–16], i.e. much shorter than the characteristic time scale of our experiments. Thus, while this distribution is not directly measurable, we expect the distribution of collective excitations in the BEC to be characterised by a temperature T_0 that is also close to $T^{\rm eq} \approx T^f$.

These conclusions hold for any $a \gtrsim 1\,a_0$ [16]. Exactly at $a = 0$ our theoretical picture does break down, since the Landau damping rate vanishes and the BEC has no equilibrium features; the two components are simply completely decoupled. Bearing this small caveat in mind, from here on we refer to $T_0 \approx T^f \approx T^{\rm eq}$ simply as the temperature of the system T.

If superheated water is perturbed, e.g., by sprinkling some salt into it, it rapidly boils away. Here, an analogous way to directly see that the gas is superheated is to suddenly increase the coupling of the BEC to the thermal bath. In Fig. 3 we show the results of two experimental series in which a is quenched (within 10 ms) from $3\,a_0$ to $62\,a_0$ at different times in the superheated regime. The solid (open) symbols show N_0 measured before (after) the quench. The small Γ_0 is essentially unaffected by the change in a, and the sudden N_0 decay is due to the increase in κ [see Fig. 1(b)]. For reference, the green line shows the calculated $N_0^{\rm eq}$ at $3\,a_0$ and orange shading indicates the superheated regime.

As shown in Fig. 4, we have explored the limits of superheating for a range of interaction strengths, including small negative values of a. For $a < 0$, a BEC is stable against collapse only for $N_0 < -C/a$, with $C \approx 2 \times 10^4\,a_0$ for our trap parameters [23–25]. However, after N_0 drops below this critical value, at small $|a|$ it decays slowly.

In Fig. 4(a) we plot the highest temperature at which we still observe a BEC, $\bar{T} \equiv T(t = \bar{t})$, scaled to the equilibrium T_c at the same N. For $a \to 0$, the BEC survives up to $T \approx 1.47\,T_c$. (For comparison, this is analogous to superheated water at 275 °C.)

In Fig. 4(b) we reconstruct the temporal phase diagram of our non-equilibrium gas. Here, a horizontal cut through the graph corresponds to a time series such as shown in Fig. 2. For each a, we plot the measured $\bar{t}$ (red points) and the equilibrium t_c (green points). The solid curves are spline fits to the data. The width of the orange-shaded region corresponds to the time that the BEC survives in the superheated regime. For $a \approx 0$

this region spans a whole minute.

The phase diagram in Fig. 4(b) is measured by always starting with $N_0 \approx 2\times10^4$. In general, non-equilibrium behaviour can strongly depend on the initial conditions. However, we find that $\bar{t}$ is essentially constant (within experimental errors) for initial N_0 in the range $(1-5)\times10^4$. The primary reason for this is that the three-body contribution to Γ_0 grows with N_0; this leads to "self-stabilisation" of the condensed atom number on timescales much shorter than $\bar{t}$.

We theoretically reproduce our non-equilibrium observations using a two-component model directly corresponding to Fig. 1(b). Starting with the measured initial N_0, we numerically simulate the evolution of a BEC coupled to a thermal bath characterised by $\mu'(t)$. To do this we calculate Γ_0 from our experimental parameters, and for κ we use the form [27]

$$\kappa = A\gamma_{\rm el}N_0\left[e^{\beta(\mu_0-\mu_c)} - e^{\beta(\mu'-\mu_c)}\right]. \qquad (1)$$

Here $\gamma_{\rm el} \propto a^2$ is the elastic collision rate and A is a dimensionless coefficient. The largest uncertainty in our calculations comes from the theoretical uncertainty in $A \approx 1-10$ [28]. (For details see Supplementary Information [16].)

In Fig. 4(a) we show the calculated $\bar{T}/T_c$. The red line corresponds to $A = 3$ and the shaded area to the range $A = 1-10$. The calculation generally captures our experimental observations well. With $A = 3$ we obtain quantitative agreement with the data, except exactly at $a = 0$, where the model is not valid. In the inset of Fig. 4(b) we show the calculated temporal phase diagram, with $A = 3$, together with the experimental $\bar{t}$ data. Again the general features of the diagram are captured well for $a \neq 0$.

In conclusion, we have observed superheating in a Bose-condensed gas with tuneable interactions, mapped out a non-equilibrium phase diagram of this system, and reproduced our measurements in numerical simulations based on a two-fluid picture of a partially condensed gas. The success of our calculations supports a conceptually simple way to think about dynamical non-equilibrium effects near a continuous phase transition. Extending the BEC lifetime by tuning interactions could also have practical benefits for precision measurements and quantum information processing.

[1] Polkovnikov, A., Sengupta, K., Silva, A. & Vengalattore, M. *Colloquium*: Nonequilibrium dynamics of closed interacting quantum systems. *Rev. Mod. Phys.* **83**, 863–883 (2011).

[2] Kinoshita, T., Wenger, T. & Weiss, D. S. A quantum Newton's cradle. *Nature* **440**, 900–903 (2006).

[3] Winkler, K. *et al.* Repulsively bound atom pairs in an optical lattice. *Nature* **441**, 853–856 (2006).

[4] Sadler, L. E., Higbie, J. M., Leslie, S. R., Vengalattore, M. & Stamper-Kurn, D. M. Spontaneous symmetry breaking in a quenched ferromagnetic spinor Bose–Einstein condensate. *Nature* **443**, 312–315 (2006).

[5] Hofferberth, S., Lesanovsky, I., Fischer, B., Schumm, T. & Schmiedmayer, J. Non-equilibrium coherence dynamics in one-dimensional Bose gases. *Nature* **449**, 324–327 (2007).

[6] Haller, E. *et al.* Realization of an excited, strongly correlated quantum gas phase. *Science* **325**, 1224–1227 (2009).

[7] Guzman, J. *et al.* Long-time-scale dynamics of spin textures in a degenerate $F = 1$ ^{87}Rb spinor Bose gas. *Phys. Rev. A* **84**, 063625 (2011).

[8] Cheneau, M. *et al.* Light-cone-like spreading of correlations in a quantum many-body system. *Nature* **481**, 484–487 (2012).

[9] Trotzky, S. *et al.* Probing the relaxation towards equilibrium in an isolated strongly correlated one-dimensional Bose gas. *Nature Physics* **8**, 325–330 (2012).

[10] Mark, M. J. *et al.* Preparation and spectroscopy of a metastable Mott-insulator state with attractive interactions. *Phys. Rev. Lett.* **108**, 215302 (2012).

[11] Smith, R. P., Beattie, S., Moulder, S., Campbell, R. L. D. & Hadzibabic, Z. Condensation dynamics in a quantum-quenched Bose gas. *Phys. Rev. Lett.* **109**, 105301 (2012).

[12] Gring, M. *et al.* Relaxation and pre-thermalization in an isolated quantum system. *Science* **337**, 1318–1322 (2012).

[13] Mathey, L. & Polkovnikov, A. Light cone dynamics and reverse Kibble-Zurek mechanism in two-dimensional superfluids following a quantum quench. *Phys. Rev. A* **81**, 033605 (2010).

[14] Fedichev, P. O., Shlyapnikov, G. V. & Walraven, J. T. M. Damping of low-energy excitations of a trapped Bose–Einstein condensate at finite temperatures. *Phys. Rev. Lett.* **80**, 2269 (1998).

[15] Pethick, C. & Smith, H. *Bose–Einstein Condensation in Dilute Gases* (Cambridge University Press, Cambridge, 2002).

[16] Online supplementary information.

[17] Campbell, R. L. D. *et al.* Efficient production of large ^{39}K Bose–Einstein condensates. *Phys. Rev. A* **82**, 063611 (2010).

[18] Roati, G. *et al.* ^{39}K Bose–Einstein condensate with tunable interactions. *Phys. Rev. Lett.* **99**, 010403 (2007).

[19] Smith, R. P., Campbell, R. L. D., Tammuz, N. & Hadzibabic, Z. Effects of interactions on the critical temperature of a trapped Bose gas. *Phys. Rev. Lett.* **106**, 250403 (2011).

[20] Tammuz, N. *et al.* Can a Bose gas be saturated? *Phys. Rev. Lett.* **106**, 230401 (2011).

[21] Smith, R. P. & Hadzibabic, Z. Effects of interactions on Bose-Einstein condensation of an atomic gas. *arXiv:1203.2063* (2012).

[22] Dalfovo, F., Giorgini, S., Pitaevskii, L. P. & Stringari, S. Theory of Bose–Einstein condensation in trapped gases. *Rev. Mod. Phys.* **71**, 463–512 (1999).

[23] Ruprecht, P. A., Holland, M. J., Burnett, K. & Edwards, M. Time–dependent solution of the nonlinear Schrödinger equation for Bose-condensed trapped neutral atoms. *Phys. Rev. A* **51**, 4704–4711 (1995).

[24] Gerton, J. M., Strekalov, D., Prodan, I. & Hulet, R. G. Direct observation of growth and collapse of a Bose–Einstein condensate with attractive interactions. *Nature* **408**, 692–695 (2000).

[25] Donley, E. A. *et al.* Dynamics of collapsing and exploding Bose–Einstein condensates. *Nature* **412**, 295–299 (2001).

[26] Smith, R. P., Tammuz, N., Campbell, R. L. D., Holzmann, M. & Hadzibabic, Z. Condensed fraction of an atomic Bose gas induced by critical correlations. *Phys. Rev. Lett.* **107**, 190403 (2011).

[27] Gardiner, C. W., Zoller, P., Ballagh, R. J. & Davis, M. J. Kinetics of Bose–Einstein condensation in a trap. *Phys. Rev. Lett.* **79**, 1793–1796 (1997).

[28] Gardiner, C. W., Lee, M. D., Ballagh, R. J., Davis, M. J. & Zoller, P. Quantum kinetic theory of condensate growth: comparison of experiment and theory. *Phys. Rev. Lett.* **81**, 5266–

5269 (1998).

* These two authors contributed equally.
† rps24@cam.ac.uk

Acknowledgements
We thank S. Beattie and S. Moulder for experimental assistance. This work was supported by EPSRC (Grant No. EP/K003615/1), the Royal Society, AFOSR, ARO and DARPA OLE.

Author Contributions
All authors contributed extensively to this work.

Additional Information
The authors declare no competing interests. Correspondence and requests for materials should be addressed to R. P. S.

Supplementary Information

Determination of N, E and N_0

We take an absorption image of the atom cloud after $\tau = 18$ ms of time-of-flight (TOF) expansion from a nearly isotropic trap with a geometric mean of trapping frequencies $\bar{\omega}/2\pi \approx 70$ Hz.

For absolute calibration of our atom numbers we use a T_c measurement at $a = 62\,a_0$, assuming that at this a the cloud is in equilibrium [1, 2].

For $a < 100\,a_0$ we assess the interaction-energy contribution to the total energy E to be $\lesssim 1\%$ and thus $E \approx 2E_k$, where E_k is the kinetic energy. We obtain E_k from the second moment of the atom distribution after TOF, and correct it for the small effect of the initial in-trap cloud size. This amounts to rescaling the energy by a factor $\bar{\omega}^2\tau^2/(1+\bar{\omega}^2\tau^2)$.

In Fig. S5 we show N and E_k for the same two experimental series shown in Fig. 2 in the main text.

To improve the detection of small N_0 values we always switch a to zero at the start of TOF [1].

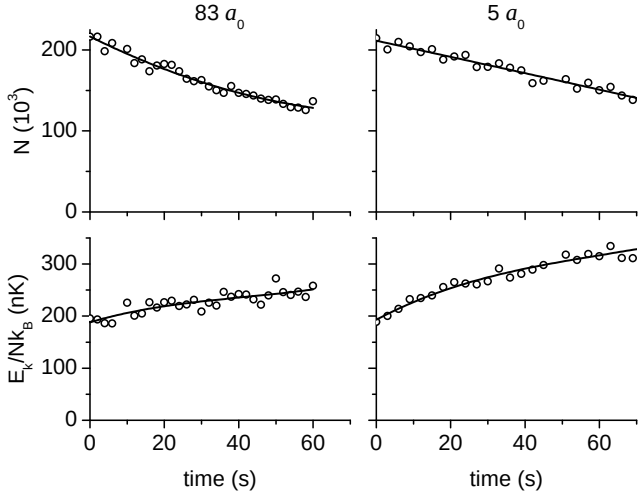

Fig. S5: **Parametrization of N and E_k.** The total atom number N and kinetic energy per particle E_k/N for two experimental series at $83\,a_0$ and $5\,a_0$. The experimental data are fitted with polynomial forms to obtain smooth functions $N(t)$ and $E_k(t)$.

Equilibrium calculations

For an equilibrium ideal Bose gas in a spherically symmetric harmonic trap of frequency ω, the thermal component satisfies:

$$N'(\mu', T) = \frac{N_c^0}{\zeta(3)} \int_0^\infty \mathrm{g}_2\left(\exp\left(\frac{\mu' - \mu_c^0}{k_\mathrm{B}T} - \frac{x^2}{2}\right)\right) x\mathrm{d}x, \tag{2}$$

$$\frac{E_k(\mu', T)}{N'(\mu', T)} = \frac{3}{2}k_\mathrm{B}T \frac{\int_0^\infty \mathrm{g}_2\left(\exp(\frac{\mu'-\mu_c^0}{k_\mathrm{B}T} - \frac{x^2}{2})\right)\frac{x^2}{2}x\mathrm{d}x}{\int_0^\infty \mathrm{g}_2\left(\exp(\frac{\mu'-\mu_c^0}{k_\mathrm{B}T} - \frac{x^2}{2})\right)x\mathrm{d}x}, \tag{3}$$

where $N_c^0 = \zeta(3)\left(\frac{k_\mathrm{B}T}{\hbar\omega}\right)^3\left(1 - \frac{\zeta(2)}{2\zeta(3)}\frac{\hbar\omega}{k_\mathrm{B}T}\right)^{-3}$ includes the finite size correction, $\mu_c^0 = \frac{3}{2}\hbar\omega$, and $\mathrm{g}_2(z)$ is the dilogarithm function. For $N > N_c^0$, the chemical potential is capped at $\mu' = \mu_c^0$ and also $\mu_0 = \mu_c^0$. The thermal atom number is saturated, $N' = N_c^0$, and any additional particles must go into the condensate, $N_0 = N - N_c^0$.

Interactions modify this picture in two ways:

(i) The critical point is shifted. At mean-field (MF) level $\mu_c = \mu_c^0 + 4\zeta(3/2)a/\lambda$, where $\lambda = \sqrt{\frac{2\pi\hbar^2}{mk_{\rm B}T}}$ is the thermal wavelength. A small beyond-MF correction is quadratic in a/λ and has an additional logarithmic correction. Experimentally, the corresponding N_c is [1, 2]

$$N_c = N_c^0 \left(1 - 3.426\frac{a}{\lambda} + 42\left(\frac{a}{\lambda}\right)^2\right)^{-3} . \tag{4}$$

(ii) Due to interactions, in the presence of a BEC, N' is no longer saturated at N_c. Empirically,

$$N' = N_c + S_0(N_0)^{2/5} + S_2(N_0)^{4/5}, \tag{5}$$

where the non-saturation parameters S_0 and S_2 depend on a and T [3, 4]. The excess number of thermal atoms, $N' - N_c$, can be directly attributed to the shift of the chemical potential above μ_c; for an interacting BEC $\mu_0 > \mu_c$ and in equilibrium $\mu' = \mu_0$.

For μ_0 we use a modified Thomas-Fermi law [5]:

$$\mu_0 - \mu_c = \frac{\hbar\omega}{2}\left\{\left(15\frac{N_0 a}{a_{\rm osc}} + 3^{5/2}\right)^{2/5} - 3\right\}, \tag{6}$$

where $a_{\rm osc} = \sqrt{\hbar/m\omega}$ is the harmonic oscillator length.

Eq. (6) and Eqs. (2) and (3) modified to include interaction effects ($N_c^0 \to N_c$ and $\mu_c^0 \to \mu_c$) form a complete set needed for our calculations [6]. We proceed in two ways:

(1) Assuming that the system is in global equilibrium, $\mu' = \mu_0 = \mu^{\rm eq}$, we use *only* $N(t)$ and $E(t)$ to calculate $\mu^{\rm eq}(t)$, $N_0^{\rm eq}(t)$ (green lines in main-text Fig. 2) and $T^{\rm eq}(t)$.

(2) Additionally, from N, E and the *measured* N_0 we calculate μ_0 and μ' without assuming $\mu' = \mu_0$ (red and blue points in the bottom panel of main-text Fig. 2).

Justification of the two-fluid picture for a gas out of global equilibrium

In our theoretical picture (Fig. 1(b) in the paper), we assume that in the superheated regime the thermal and condensed components can still to a good approximation be assumed to be separately in equilibrium. Moreover, we assume that they are at the same temperature, but just have different chemical potentials.

Here we provide a more detailed justification of these assumptions.

First, for the thermal component we show in Fig. S6 that the radial velocity distribution still looks like a thermal distribution at a temperature very close to the calculated $T^{\rm eq}(N, E)$. Here we show data for the same 5 a_0 series as shown in Fig. 2(b) in the main paper. In Fig. S6(a) we show the distribution measured at $t = 45$ s, i.e. deep in the superheated regime. The data (red) is fitted almost perfectly by an equilibrium thermal distribution constrained to be characterised by N, E and $T^{\rm eq}$ (green). An unconstrained fit (blue) gives only a very slightly different shape with T^f within few % of $T^{\rm eq}$. In Fig. S6(b) we compare the calculated $T^{\rm eq}$ (green) and the fitted T^f (blue) for the whole 5 a_0 series. For comparison we also show the equilibrium T_c (black line). Note that this is the same plot as in Fig. 2(b) in the main paper, with just the T^f points added.

Second, for the collective excitations in the BEC to be in equilibrium with the thermal bath, the Landau-damping time τ_L [7, 8] must be short compared to the characteristic time scale of the experiment. For a uniform system at a temperature higher than the interaction energy per particle [8]:

$$\frac{\tau_L\omega}{2\pi} \approx \frac{n_0^{1/2}\lambda_T^2}{4\pi a^{1/2}}, \tag{7}$$

where ω is the excitation frequency, n_0 is the condensate density, and λ_T is the thermal wavelength. For our assessment we use this uniform-system result with our peak n_0; this only overestimates τ_L for a harmonically trapped gas [7].

Exactly at $a = 0$ the damping time diverges and our theoretical picture breaks down. However, already for $a = 1$ a_0, for all our experimental parameters the RHS of Eq. (7) is < 100. Then, even for our lowest-energy modes, with $\omega/2\pi \sim 100$ Hz, we get $\tau_L < 1$ s.

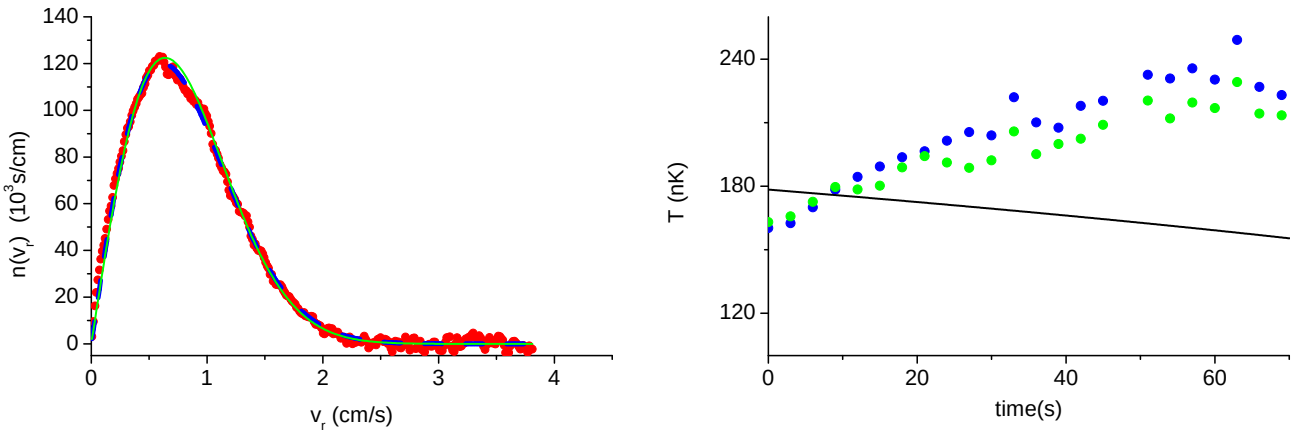

Fig. S6: **Thermal distribution in a gas out of global phase equilibrium**. (a) For a gas at 5 a_0 in the superheated regime we show the radial velocity distribution (red), the distribution corresponding to N, E and $T^{\rm eq}$ (green) and the unconstrained fit (blue) giving T^f. Even though the gas is not in true global equilibrium the distribution still looks thermal and T^f and $T^{\rm eq}$ agree to within few %. (b) Comparison of T^f (blue) and $T^{\rm eq}$ (green) for the whole 5 a_0 data series shown in Fig. 2(b) of the main paper. The solid black line shows the equilibrium T_c.

Non-equilibrium evolution of N_0

The non-equilibrium evolution of N_0 is described by the differential equation

$$\dot{N_0} = -\kappa - \Gamma_0 N_0 \,, \tag{8}$$

where κ is the coupling to the thermal bath due to elastic collisions and Γ_0 is the instantaneous inelastic loss rate per particle. Following [9] we use

$$\kappa = A\frac{8m(ak_{\rm B}T)^2}{\pi\hbar^3}e^{2\beta(\mu'-\mu_c)}\left[e^{\beta(\mu_0-\mu')}-1\right]N_0 = A\gamma_{\rm el}N_0\left[e^{\beta(\mu_0-\mu_c)}-e^{\beta(\mu'-\mu_c)}\right] , \tag{9}$$

where $\gamma_{\rm el} = \frac{8m(ak_{\rm B}T)^2}{\pi\hbar^3}e^{\beta(\mu'-\mu_c)}$ is essentially the elastic scattering rate for a thermal cloud at μ' and $A \approx 1-10$ is a theoretically uncertain prefactor [5].

In the inelastic loss term we include contributions from one-body scattering and three-body recombination, $\Gamma_0 = \Gamma_0^{(1)} + \Gamma_0^{(3)}$. In our system, one-body loss is dominated by spontaneous scattering of photons from the trapping laser beams. We calculate it from the known wavelength and intensity of the beams. For all the reported experiments

$$\Gamma_0^{(1)} \approx \frac{1}{35}{\rm s}^{-1} . \tag{10}$$

The loss rate of condensate atoms due to three-body recombination in the presence of a thermal cloud is given by [10]

$$\Gamma_0^{(3)} = \frac{K_3(a)}{6}\left(\langle n_0^2\rangle + 6\langle n_0 n'\rangle + 6\langle n'^2\rangle\right) , \tag{11}$$

where n_0 is the condensate density, n' the thermal density, $K_3(a)$ the known a-dependant three-body coefficient [11, 12], and $\langle ...\rangle$ stands for an average over the density distribution. We set n' to its value in the centre of the trap and for the condensate we again use a modified Thomas-Fermi approach:

$$\langle n_0\rangle = \frac{\langle n_0\rangle_{\rm GS}}{\left[1+\left(\langle n_0\rangle_{\rm GS}/\langle n_0\rangle_{\rm TF}\right)^{5/3}\right]^{3/5}} , \tag{12}$$

$$\langle n_0^2\rangle = \frac{\langle n_0^2\rangle_{\rm GS}}{\left[1+\left(\langle n_0^2\rangle_{\rm GS}/\langle n_0^2\rangle_{\rm TF}\right)^{5/6}\right]^{6/5}} . \tag{13}$$

Here GS refers to the non-interacting Gaussian ground state and TF to the Thomas-Fermi approximation, $\langle n_0\rangle_{\rm TF} = \sqrt{2\pi}(15/7)(15N_0a/a_{\rm osc})^{-3/5}\langle n_0\rangle_{\rm GS}$ and $\langle n_0^2\rangle_{\rm TF} = \sqrt{3}\pi(15^2/56)(15N_0a/a_{\rm osc})^{-6/5}\langle n_0^2\rangle_{\rm GS}$, where $\langle n_0\rangle_{\rm GS} = N_0/(2\pi a_{\rm osc}^2)^{3/2}$ and $\langle n_0^2\rangle_{\rm GS} = N_0^2/(3\pi^2 a_{\rm osc}^4)^{3/2}$. Eqs. (12) and (13) smoothly interpolate between the ground state result (for $N_0a/a_{\rm osc} \ll 1$) and the Thomas-Fermi approximation (for $N_0a/a_{\rm osc} \gg 1$). Note that other forms which smoothly interpolate between these two limits give essentially the same results.

Using Eqs. (8) - (13) we simulate the evolution of the condensate atom number, $N_0(t)$, from its initial value $N_0(t=0)$. We use the measured $N(t)$ and $E(t)$ and the numerically evolved $N_0(t)$ to obtain $\mu'(t)$ for use in Eq. (9). To determine $\bar{t}$ from our calculations we define the condensate to be present if N_0 is larger than $N_0^{\rm min} = 3k_{\rm B}T/(\hbar\omega)$, the thermal occupation of the first excited state.

In the main text we show the results of our calculations for $\bar{T}$ and $\bar{t}$ (Fig. 4), with $A = 3$. In Fig. S7 we show that our calculations (with the same value of A) also describe well the full dynamics $N_0(t)$.

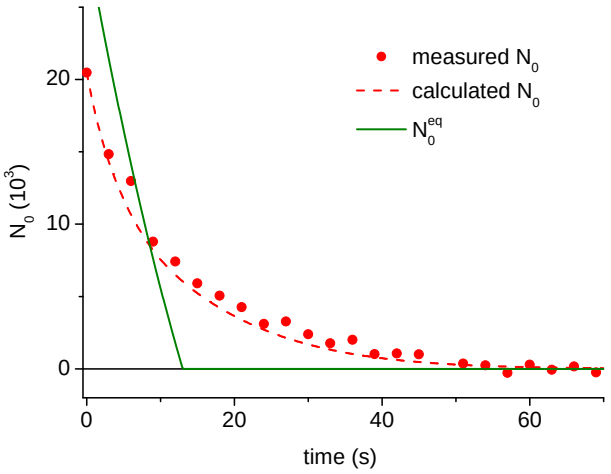

Fig. S7: **Non-equilibrium N_0 dynamics**. We plot the calculated $N_0(t)$ (dashed red line) together with the measured N_0 (red points) for the same $5\,a_0$ data series as in Fig. 2(b) in the main text. For comparison we also show the calculated $N_0^{\rm eq}(t)$ (solid green line).

[1] Smith, R. P., Campbell, R. L. D., Tammuz, N. & Hadzibabic, Z. Effects of interactions on the critical temperature of a trapped Bose gas. *Phys. Rev. Lett.* **106**, 250403 (2011).

[2] Smith, R. P., Tammuz, N., Campbell, R. L. D., Holzmann, M. & Hadzibabic, Z. Condensed fraction of an atomic Bose gas induced by critical correlations. *Phys. Rev. Lett.* **107**, 190403 (2011).

[3] Tammuz, N. *et al.* Can a Bose gas be saturated? *Phys. Rev. Lett.* **106**, 230401 (2011).

[4] Smith, R. P. & Hadzibabic, Z. Effects of interactions on Bose-Einstein condensation of an atomic gas. *arXiv:1203.2063* (2012).

[5] Gardiner, C. W., Lee, M. D., Ballagh, R. J., Davis, M. J. & Zoller, P. Quantum kinetic theory of condensate growth: comparison of experiment and theory. *Phys. Rev. Lett.* **81**, 5266–5269 (1998).

[6] In Eqs. (2) and (3) we also replace the function g_2 with a slightly modified dilogarithm function $\tilde{\mathrm{g}}(z) = (3/4)|\mathrm{g}_2(z)| + (1/4)\mathrm{Re}\{\mathrm{g}_2(z)\}$, which remains real for $z > 1$. This is done just for mathematical convenience and does not affect our results since the integrals are strongly dominated by the region where $x^2/2 > (\mu' - \mu_{\rm c})/k_{\rm B}T$ and $\tilde{\mathrm{g}} = \mathrm{g}_2$.

[7] Fedichev, P. O., Shlyapnikov, G. V. & Walraven, J. T. M. Damping of low-energy excitations of a trapped Bose–Einstein condensate at finite temperatures. *Phys. Rev. Lett.* **80**, 2269 (1998).

[8] Pethick, C. & Smith, H. *Bose–Einstein Condensation in Dilute Gases* (Cambridge University Press, Cambridge, 2002).

[9] Gardiner, C. W., Zoller, P., Ballagh, R. J. & Davis, M. J. Kinetics of Bose–Einstein condensation in a trap. *Phys. Rev. Lett.* **79**, 1793–1796 (1997).

[10] Söding, J. *et al.* Three-body decay of a rubidium Bose–Einstein condensate. *Appl. Phys. B* **69**, 257 (1999).

[11] Zaccanti, M. *et al.* Observation of an Efimov spectrum in an atomic system. *Nature Physics* **5**, 586–591 (2009).

[12] Zaccanti, M. *Tuning of the interactions in ultracold K-Rb quantum gases*. Ph.D. thesis, University of Florence (2007).